Received: 11 May 2022 | Revised: 5 August 2022 | Accepted: 25 August 2022

DOI: 10.1002/ecy.3877

ARTICLE

ECOLOGY
ECOLOGICAL SOCIETY OF AMERICA

Embolism resistance explains mortality and recovery of five subtropical evergreen broadleaf trees to persistent drought

Junjiong Shao[1,2] | **Xuhui Zhou**[1,3] | **Peipei Zhang**[1,4] | **Deping Zhai**[1,5] | **Tengfei Yuan**[1,6] | **Zhen Li**[1] | **Yanghui He**[1,3] | **Nate G. McDowell**[7,8]

[1]Center for Global Change and Ecological Forecasting, Tiantong National Field Observation Station for Forest Ecosystem, School of Ecological and Environmental Sciences, East China Normal University, Shanghai, China

[2]State Key Laboratory of Subtropical Silviculture, Zhejiang A&F University, Hangzhou, China

[3]Northeast Asia ecosystem Carbon sink research Center (NACC), Center for Ecological Research, Key Laboratory of Sustainable Forest Ecosystem Management-Ministry of Education, School of Forestry, Northeast Forestry University, Harbin, China

[4]CAS Key Laboratory of Mountain Ecological Restoration and Bioresource Utilization & Ecological Restoration and Biodiversity Conservation Key Laboratory of Sichuan Province, Chengdu Institute of Biology, Chinese Academy of Sciences, Chengdu, China

[5]School of Ecology and Environmental Science, Yunnan University, Kunming, China

[6]School of Atmospheric Sciences, Nanjing University, Nanjing, China

[7]Atmospheric Sciences and Global Change Division, Pacific Northwest National Lab, Richland, Washington, USA

[8]School of Biological Sciences, Washington State University, Pullman, Washington, USA

Correspondence
Xuhui Zhou
Email: xhzhou@des.ecnu.edu.cn

Funding information
Department of Energy's Next Generation Ecosystem Experiment (NGEE)-Tropics project; National Key R&D Program of China, Grant/Award Number: 2017YFA06046; National Natural Science Foundation of China, Grant/Award Numbers: 31930072, 31600387

Handling Editor: Joseph B. Yavitt

Abstract

Subtropical evergreen broadleaf forests (SEBF) are experiencing and expected to suffer more frequent and severe drought events. However, how the hydraulic traits directly link to the mortality and recovery of SEBF trees remains unclear. In this study, we conducted a drought–rewatering experiment on tree seedlings of five dominant species to investigate how the hydraulic traits were related to tree mortality and the resistance and recovery of photosynthesis (A) and transpiration (E) under different drought severities. Species with greater embolism resistance (P_{50}) survived longer than those with a weaker P_{50}. However, there was no general hydraulic threshold associated with tree mortality, with the lethal hydraulic failure varying from 64% to 93% loss of conductance. The photosynthesis and transpiration of tree species with a greater P_{50} were more resistant to and recovered faster from drought than those with lower P_{50}. Other plant traits could not explain the interspecific variation in tree mortality and drought resistance and recovery. These results highlight the unique importance of embolism resistance in driving carbon and water processes under persistent drought across different trees in SEBFs. The absence of multiple efficient drought strategies in SEBF seedlings implies the difficulty of natural seedling regeneration under future droughts, which often occurs after destructive disturbances (e.g., extreme drought events and typhoon),

suggesting that this biome may be highly vulnerable to co-occurring climate extremes.

KEYWORDS
drought–rewatering, embolism resistance, PLC threshold, recovery, subtropical forest, tree mortality

INTRODUCTION

Forest ecosystems are critical to global biodiversity and the carbon sink (Pan et al., 2013). However, in the context of climate change, more frequent and severe drought events have induced substantial forest mortality and hampered ecosystem functions (Hartmann et al., 2018; McDowell et al., 2022). As two paramount functions, the carbon and water dynamics are key processes mediating the feedbacks between forests and the climate system (Haughton et al., 2018). Unfortunately, forecasting the carbon and water fluxes under drought suffers great uncertainty (Vargas et al., 2013), largely due to the insufficient understanding on the resilience of tree physiological processes (e.g., photosynthesis and transpiration).

Two measurable components of resilience are resistance and recovery, which quantify the impact of an exogenous disturbance on a system and the rate and magnitude of recovery, respectively (Hodgson et al., 2015). Previous studies showed that species-level differences in resistance to drought (Anderegg et al., 2016; Roman et al., 2015) could be attributed to differences in hydraulic processes. For example, photosynthesis (A) and transpiration (E) of relatively isohydric plants (i.e., small declines in midday water potential despite drying soil) may be highly sensitive to drought because they closed stomata more rapidly than relatively anisohydric plants (Martínez-Vilalta et al., 2014). In contrast, species with higher embolism resistance or deeper rooting depths are able to maintain higher water potential and hydraulic conductance, suggesting that their physiological rates (e.g., A and E) are more resistant to severe drought (Meinzer & McCulloh, 2013). In addition, plants with greater turgor loss point (π_{tlp}) in leaves were more tolerant to internal water limitations, thereby buffering stomata closure (Zhu et al., 2018). These hydraulic characteristics may be coordinated with each other, and correlated with other functional traits, as a result of coselections on plant traits (Bartlett et al., 2016; Mursinna et al., 2018). However, there are also studies showing decoupling between them (Kannenberg et al., 2019; Li, Feifel, et al., 2015), which raises the question of whether multiple plant traits would coregulate the drought resistance in forests.

The extreme impact of drought on tree physiology may ultimately trigger death (McDowell et al., 2013). A tipping point of hydraulic failure may occur after trees die (Hammond et al., 2019; Urli et al., 2013). However, the exact extent of hydraulic failure inducing tree mortality varies among studies, with values from 50% loss of stem conductance (PLC) to >80% PLC (Brodribb et al., 2010; Hammond et al., 2019; Kursar et al., 2009; McDowell et al., 2013; Urli et al., 2013). This large variation of lethal stem PLC might reflect the complex mechanisms with two issues: whether trees can recover through embolism refilling or new xylem growth after drought (Gauthey et al., 2022) and whether the hydraulic systems in leaves and roots are more vulnerable to drought than that in stems (Creek et al., 2018; Levionnois et al., 2020). Although the concept of a point of no return of hydraulic failure has been widely adopted, a common value of PLC causing tree death has not emerged.

Compared to research on drought resistance and mortality, those focusing on the role of plant traits in regulating postdrought recovery are relatively rare, and conclusions are more uncertain. Among a few studies, some showed that a higher level of xylem embolism limited postdrought recovery (Peguero-Pina et al., 2018; Urli et al., 2013), whereas others suggested that plants with lower embolism resistance may have a greater ability to repair embolisms (Klein et al., 2018). Similarly, on the one hand, relatively isohydric plants might show more rapid postdrought recovery of photosynthesis than anisohydric plants due to the lower risk of hydraulic failure (Kannenberg et al., 2019). On the other hand, isohydric plants could also exhibit slow postdrought recovery (Garcia-Forner et al., 2016) because they have lower photosynthate, which provides energy for the signaling of stomatal response, osmotic adjustments, and embolism refilling, than anisohydric plants under drought stress (Klein et al., 2018; Pou et al., 2012). Therefore, whether a particular trait would regulate the recovery of photosynthesis and transpiration needs to be confirmed by experiments designed to investigate the resilience of tree physiology.

Subtropical evergreen broadleaf forests (SEBFs), which have a large distribution in southern China, are global hotspots for biodiversity and carbon sequestration

(Fan et al., 2018; Yu et al., 2014). Historical observations and model forecasting suggest that southern China has suffered and will experience more severe, frequent, and extensive droughts (Dai, 2013; Yuan et al., 2016). Historically, the selection pressure induced by water deficit in SEBFs is not as strong as that in arid ecosystems. Therefore, the mechanisms underlying the drought resistance and resilience of SEBF species may be different from those underlying the species grown in arid biomes such as Mediterranean forests or arid grasslands.

To explore the mechanisms driving interspecific differences in drought resistance and resilience among SEBF species, we performed a common garden drought–rewatering experiment on seedlings of five dominant species with differential drought sensitivities at a SEBF in China. A drought gradient was created by withholding water for different numbers of days (8, 14, 20, 26, 32, 38, and 44 days). To understand recovery dynamics, a subset of plants was rewatered for each level of drought gradient after the corresponding number of days of water withholding. Plant morphological, photosynthetic, and hydraulic traits were examined in relation to the response and recovery of photosynthesis and transpiration. Our main objectives were (1) to explore which plant traits explained the interspecific differences in tree mortality and drought resistance and recovery and (2) to investigate whether a general PLC threshold for tree death exists among the studied trees.

METHODS

Study site and experimental design

The experiment was carried out in a common garden located in Ningbo, Zhejiang Province, China (29.86° N, 121.34° E). This region is characterized by hot, wet summers and cool, dry winters. The mean annual temperature and precipitation were 16.2°C and 1374 mm, respectively. Precipitation occurs primarily from May to August, but there are heat weaves and extreme droughts during this period in some years. In 2017, there was no rainfall during the entire August, resulting in an extremely dry summer. The natural vegetation is subtropical evergreen broadleaf forest, with a growing season from May to October. Soils were mainly red or yellow earths with a high abundance of iron and aluminum oxides as an Acrisol soil. The substrate of parental material was mesozoic sediments and acidic intrusive rocks. Soil pH was 4.4–5.1, and texture was a clay loam (6.8% sand, 55.5% silt, and 4.7% clay; Yan et al., 2006).

Five dominant tree species were selected (*Cyclobalanopsis gilva*, *Castanopsis sclerophylla*, *Neocinnamomum chekiangense*, *Phoebe chekiangensis*, and *Schima superba*). According to previous observations, *C. sclerophylla* and *S. superba* were relatively insensitive, whereas *P. chekiangensis* was highly sensitive to water deficit (Duan et al., 2019; Li et al., 2019). Overall, these species represented a wide range of drought sensitivities in the studied forest.

A total of 1250 (250 for each species) 2- to 3-year-old seedlings were transplanted from a nursery garden into 18-L plastic pots (30 cm in diameter and 25 cm in height) during 10–15 April 2017. The substrate was yellow soil with 5.6% peat, 2.0% manure, and 1.0% calcium superphosphate. The pots were located in the field with full irrigation for 3 months. On 10 July, all pots were transferred into a greenhouse covered with transparent plastic film (90% transmittance) on top but with the surrounding walls open to the atmosphere, allowing thorough cross-ventilation. The plants were fully irrigated for 2 weeks to allow maximum acclimation to their new environment. Drought treatments began on 26 July (DOY 206). For each species, there was one control group with sufficient water and seven drought–rewatering groups, with water being withheld for 8, 14, 20, 26, 32, 38, and 44 days, respectively. After each group reached its required days of drought, the plants were fully irrigated until the end of September (DOY 273). However, the measurements stopped once the trees fully recovered, died, or had no signs of further recovery after 30 days of rewetting. For the partially recovered plants, it was the end of the growing season after 30 days of rewetting, in which period the plants did not develop new leaves. These plants may fully recover in the spring of next year, but this was beyond the scope of this study. The measurements of physiological parameters and biomass during soil drying and recovery processes were made on three replications, whereas the measurements of plant traits were made on varied replications (see Table 1 for details).

Measurements of environmental variables

To continuously trace the temperature and relative humidity in the greenhouse, two hygrothermographs were located at 1.8 m in height. Two methods were used to monitor soil water content (SWC). One was the weighing method timed when there were destructive samplings. Specifically, soils at a depth of 10 cm were sampled and put in aluminum boxes for oven drying at 105°C for 24 h. The soil weights before and after oven drying were used to calculate the SWC. The other method was a portable soil moisture meter that measures SWC nondestructively. To account for systematic differences, SWC from the second method was corrected by using the linear relationship between the two methods. The relationship was $y = 1.02x - 0.35$, ($r^2 = 0.67$, $p < 0.001$).

TABLE 1 Morphological, photosynthetic, and hydraulic traits of the five species.

Trait	*Cyclobalanopsis gilva*	*Castanopsis sclerophylla*	*Neocinnamomum chekiangense*	*Phoebe chekiangensis*	*Schima superba*	*n*
Porous	Diffuse	Ring	Diffuse	Diffuse	Diffuse	
Height (cm)	67.81 ± 0.58^{B}	45.74 ± 0.44^{D}	87.80 ± 0.71^{A}	58.58 ± 0.34^{C}	60.12 ± 0.54^{C}	249
Diameter (mm)	7.24 ± 0.08^{B}	5.40 ± 0.06^{E}	8.56 ± 0.09^{A}	6.90 ± 0.05^{C}	6.21 ± 0.06^{D}	249
Root:shoot	0.75 ± 0.12	0.51 ± 0.03	0.49 ± 0.07	0.55 ± 0.06	0.48 ± 0.05	5
Leaf size (cm^2)	8.39 ± 0.58^{C}	13.76 ± 0.39^{B}	13.43 ± 0.33^{B}	20.84 ± 0.39^{A}	14.67 ± 0.80^{B}	25
SLA ($cm^2\ g^{-1}$)	124 ± 4^{A}	114 ± 8^{AB}	103 ± 3^{B}	106 ± 4^{B}	113 ± 6^{AB}	25
LDMC	0.42 ± 0.02^{AB}	0.43 ± 0.00^{A}	0.43 ± 0.02^{AB}	0.41 ± 0.01^{AB}	0.36 ± 0.02^{B}	25
Wood density ($g\ cm^{-3}$)	0.56 ± 0.03^{AB}	0.55 ± 0.02^{AB}	0.48 ± 0.03^{B}	0.51 ± 0.01^{AB}	0.61 ± 0.02^{A}	5
LA:BA	2094 ± 453	1665 ± 261	1850 ± 349	2886 ± 202	2523 ± 279	5
A_{max} (μ mol $m^{-2}\ s^{-1}$)	12.67 ± 1.08	15.43 ± 1.70	12.70 ± 1.09	14.17 ± 0.39	13.40 ± 1.06	5
K_m (μ mol $m^{-2}\ s^{-1}$)	145 ± 21	198 ± 32	155 ± 21	170 ± 16	197 ± 26	5
R_d (μ mol $m^{-2}\ s^{-1}$)	1.14 ± 0.25	1.27 ± 0.09	1.23 ± 0.25	1.15 ± 0.26	1.05 ± 0.15	5
LCP (μ mol $m^{-2}\ s^{-1}$)	14 ± 3	17 ± 2	16 ± 2	14 ± 1	17 ± 4	5
α	0.072 ± 0.005	0.070 ± 0.011	0.072 ± 0.012	0.080 ± 0.008	0.081 ± 0.007	5
V_{cmax} (μ mol $m^{-2}\ s^{-1}$)	41.99 ± 4.78	45.11 ± 4.09	37.04 ± 4.15	39.07 ± 2.01	32.75 ± 5.41	5
J_{max} (μ mol $m^{-2}\ s^{-1}$)	81.03 ± 9.45	96.81 ± 18.73	86.88 ± 21.07	82.91 ± 9.58	71.20 ± 9.73	5
J_{max}:V_{cmax}	1.96 ± 0.22	2.10 ± 0.28	2.28 ± 0.29	2.13 ± 0.22	2.22 ± 0.19	5
P_{50} (MPa)	-0.91 ± 0.08^{A}	-2.46 ± 0.11^{C}	-1.33 ± 0.07^{B}	-0.67 ± 0.13^{A}	-1.92 ± 0.12^{C}	10
P_{88} (MPa)	-2.77 ± 0.299^{AB}	-3.23 ± 0.19^{AB}	-2.27 ± 0.09^{A}	-6.80 ± 0.70^{C}	-3.94 ± 0.36^{B}	10
Ψ_{close} (MPa)	-1.80 ± 0.19	-1.80 ± 0.17	-2.50 ± 0.14	-3.13 ± 0.68	-2.29 ± 0.21	3
Ψ_{min} (MPa)	-3.94 ± 0.24	-3.53 ± 0.22	-3.50 ± 0.25	-3.50 ± 0.35	-2.85 ± 0.24	3
$HSM_{close\text{-}88}$ (MPa)	0.97 ± 0.10^{BC}	1.43 ± 0.14^{BC}	-0.23 ± 0.01^{C}	3.67 ± 0.80^{A}	1.65 ± 0.15^{B}	3
$HSM_{min\text{-}88}$ (MPa)	-1.32 ± 0.08^{D}	-0.30 ± 0.02^{C}	-1.23 ± 0.09^{D}	3.30 ± 0.33^{A}	1.09 ± 0.09^{B}	3
σ	0.64 ± 0.13	0.54 ± 0.07	0.81 ± 0.10	0.71 ± 0.11	0.69 ± 0.06	5
Λ (MPa)	-1.42 ± 0.25^{CD}	-1.69 ± 0.15^{D}	-1.10 ± 0.14^{B}	-1.37 ± 0.18^{C}	-1.00 ± 0.13^{A}	5
π_{tlp} (MPa)	-1.98 ± 0.09^{A}	-2.20 ± 0.03^{A}	-2.60 ± 0.04^{B}	-2.50 ± 0.04^{B}	-1.98 ± 0.14^{A}	5
ε (MPa)	8.94 ± 2.21^{B}	11.97 ± 1.44^{AB}	24.15 ± 1.87^{A}	17.94 ± 3.85^{AB}	10.65 ± 0.51^{B}	5
Survival time (days)	21.5 ± 1.5	29 ± 3	21.5 ± 1.5	15.5 ± 1.5	24.5 ± 1.5	

Note: The values for survival time are mean $\pm$ 0.5 $\times$ range and mean $\pm$ SE for other traits. The comparison among species was conducted by Kruskall–Wallis test for root:shoot, SLA, LDMC, LA:BA, π_{tlp}, and ε and by one-way ANOVA for other traits. No statistical test was conducted for survival time because it represents the ranges. Samples size (n) for A_{max}, K_m, R_d, LCP, α of *S. superba* is four. Sample size for V_{cmax}, J_{max}, and J_{max}:V_{cmax} of *C. gilva*, *P. chekiangensis*, and *S. superba* is four, whereas that of *N. chekiangense* is three. SLA, specific leaf area; LDMC, leaf dry matter content; LA:BA, ratio of leaf area to basal area; A_{max}, light-saturated photosynthetic rate; K_m, Michaelis constant for light response curve; R_d, dark respiration; LCP, light compensation point; α, quantum efficiency; V_{cmax}, maximum rate of carboxylation; J_{max}, maximum rate of electron transport; P_{50}, xylem water potential at 50% loss of hydraulic conductivity; P_{88}, xylem water potential at 88% loss of hydraulic conductivity; Ψ_{close}, leaf water potential causing 90% stomatal closure; Ψ_{min}, minimum leaf water potential; $HSM_{close\text{-}88}$, hydraulic safety margin from Ψ_{close} to P_{88}; $HSM_{min\text{-}88}$, hydraulic safety margin from Ψ_{min} to P_{88}; σ, isohydricity; Λ, leaf water potential at soil potential = 0; π_{tlp}, turgor loss point; ε, bulk modulus of elasticity.

Measurement of plant traits

Morphological traits

Morphological traits included plant height, basal diameter, leaf size, specific leaf area (SLA), leaf dry matter content (LDMC), leaf area:basal area ratio, wood density, and root:shoot biomass ratio. These measurements generally followed the handbook of Pérez-Harguindeguy et al. (2013). Specifically, plant height and stem diameter were measured on all plants. The ratio of leaf area to basal area, woody density, and

ratio of root to shoot were measured on five randomly selected individuals for each species. Leaf size, SLA, and LDMC were measured on five individuals with five mature leaves for each individual. These measurements were conducted before the drought treatment during 20–26 July.

Photosynthetic traits

Photosynthetic traits, including the parameters of light and CO_2 response curves of five individuals, were collected before the drought treatment using a portable photosynthesis apparatus (LI-6400; LI-COR) from 8:00 to 11:00 a.m. on sunny days. The light response curves were measured at ambient CO_2 concentration, with the temperature and relative humidity in the chamber being around 25°C and 60%, respectively. The light-intensity gradient was 1500, 1000, 500, 250, 120, 60, 40, 20, 10, and 0 μ mol m^{-2} s^{-1}. For the CO_2 response curves, the temperature, relative humidity, and light intensity in the chamber were maintained at 25°C, 60%, and 1000 μ mol m^{-2} s^{-1}, respectively. The CO_2 gradient was 400, 50, 100, 150, 200, 250, 350, 500, 700, 900, 1200, and 1400 ppm. The light-response curve was fitted by the Michaelis–Menten model (de A. Lobo et al., 2013). Light-saturated photosynthesis (A_m), Michaelis constant (K_m), dark respiration (R_d), light compensation point (LCP), and apparent quantum yield (α, ratio of A_m to K_m) were calculated. The CO_2 response curve was fitted by the FvCB model (Duursma, 2015):

$$A_m = \frac{A_c + A_j - \sqrt{(A_c + A_j)^2 - 4\theta A_c A_j}}{2\theta} - R_d, \quad (1)$$

$$A_c = \frac{V_{cmax}(C_i - \Gamma^*)}{\left[C_i + K_c\left(1 + \frac{O_i}{K_0}\right)\right]}, \quad (2)$$

$$A_j = \left(\frac{J}{4}\right) \times \frac{(C_i - \Gamma^*)}{(C_i + 2\Gamma^*)}, \quad (3)$$

where A_m is the hyperbolic minimum of Rubisco-limited (A_c) and ribulose 1,5-bisphosphate regeneration limited photosynthesis (A_j); θ is a shape parameter set to 0.9999, V_{cmax} and J_{max} are the maximum carboxylation and electron transport rates (J_{max}), respectively; C_i and O_i are the intercellular concentrations of CO_2 and O_2, respectively; K_c and K_o are the Rubisco activity for CO_2 and O_2, respectively; and Γ* is the CO_2 compensation point. The parameters V_{cmax} and J_{max} were fitted by the R package plantecophys (Duursma, 2015).

Hydraulic traits

The hydraulic traits included stem embolism resistance, leaf drought tolerance (turgor loss parameters), and relative anisohydricity before drought treatment. Specifically, stem embolism resistance (P_{50}) was derived from the stem vulnerability curves, which were measured by the air-dehydration method (Sperry et al., 1988). For each species, 10 stems were dehydrated on a bench to obtain various degrees of drought. For each drought degree, xylem water potential was measured by a pressure chamber (SAP II 3115, SEC, US), and PLC was measured using the XYL'EM hydraulic conductance and embolism measurement system (INRA, France). For PLC measurement, 20- to 30-cm stem segments were cut under a KCl solution (2 mM) (Duan et al., 2019). Of the five species, *C. gilva* and *C. sclerophylla* belong to family Fagaceae, and *N. chekiangense* and *P. chekiangensis* belong to family Lauraceae. The longest vessel length of both families was shorter than 20 cm (Jacobsen et al., 2012). *S. superba* belongs to family Theaceae, whose vessel length was not available but the stem sample of a previous study on *S. superba* was 20–30 cm (Duan et al., 2019). Therefore, the resulting vulnerability curves would not suffer the problem of shorter stems than vessel length. A reparameterized Weibull equation was used to fit the vulnerability curve (Figure 1; Ogle et al., 2009):

$$PLC = 1 - \left(1 - \frac{X}{100}\right)^{\left[\left(\frac{P}{P_X}\right)^{\frac{P_X S_X}{V}}\right]}, \quad (4)$$

$$V = (X - 100)\log\left(1 - \frac{X}{100}\right), \quad (5)$$

where P_X is the xylem potential when PLC was X, and S_X is a shape parameter. The hydraulic safety margin (HSM) was quantified by two methods. One was the $HSM_{min\text{-}88}$, the difference between the minimum leaf water potential (Ψ_{min}) and P_{88}, and the other was $HSM_{close\text{-}88}$, the difference between the leaf water potential causing 90% stomatal closure (Ψ_{close}) and P_{88}. The Ψ_{min} was the minimum observed water potential of green leaves for plants able to recover. The Ψ_{close} was determined by constructing the relationship between stomatal conductance (g_s) and predawn leaf water potential (Ψ_{PD}) in plants under the drought treatment:

$$g_s = b_1 e^{(-\Psi_{PD}/b_2)^{b_3}}. \quad (6)$$

Ψ_{close} is the Ψ_{PD} corresponding to g_s at $0.1 \times b_1$.

Drought tolerance traits π_{tlp} (leaf water potential at turgor loss point) and ε (modulus of elasticity) were

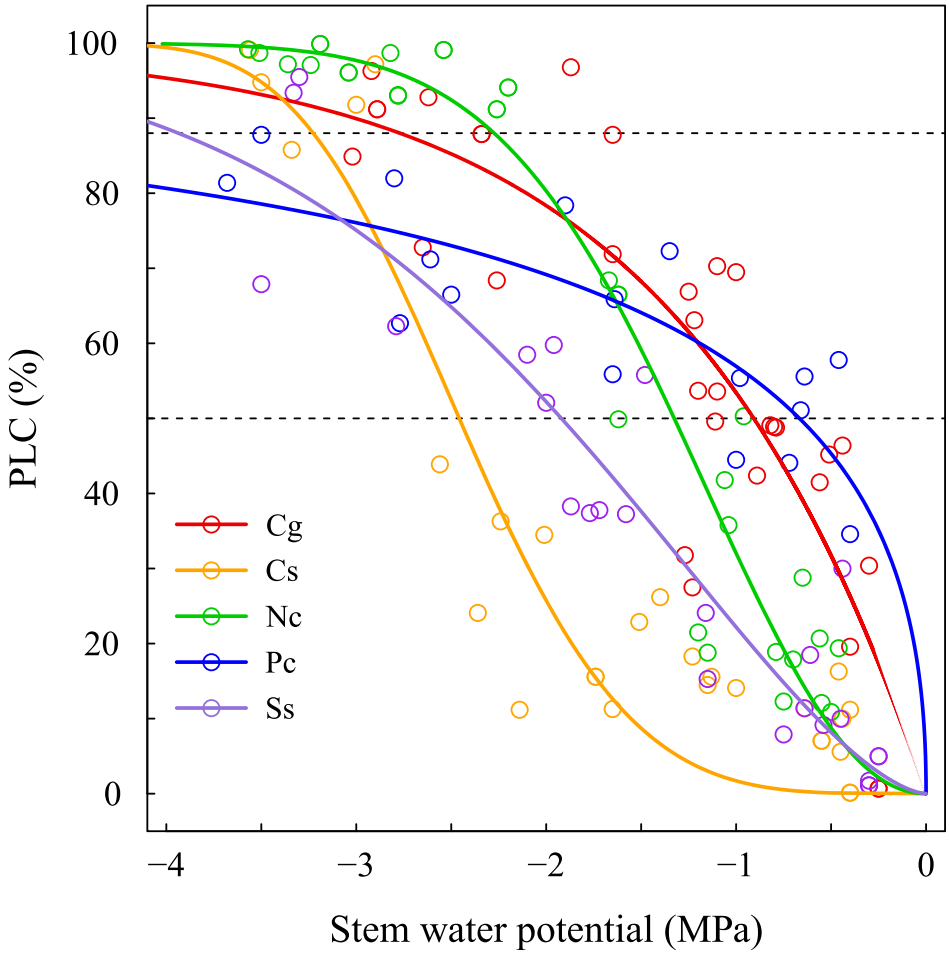

FIGURE 1 Stem vulnerability curves of the five species. The horizontal dashed lines represent 50% and 88% loss of hydraulic conductance. Cg, *Cyclobalanopsis gilva*; Cs, *Castanopsis sclerophylla*; Nc, *Neocinnamomum chekiangense*; Pc, *Phoebe chekiangensis*; Ss, *Schima superba*. PLC, percentage loss of stem conductance.

derived from pressure–volume curves, which are the relationship between leaf water potential (Ψ) and relative water content. Pressure–volume curves were measured on five leaves for each species by the squeeze method (Schulte & Hinckley, 1985). The detailed measurement followed the online procedure in Prometheus Wiki (http://prometheuswiki.org/tiki-ndex.php?page=Leaf+pressure-volume+curve+parameters).

The degree of anisohydricity (σ) was calculated as the slope of the regression line between midday (Ψ_{MD}) and predawn leaf water potentials (Ψ_{PD}; Martínez-Vilalta et al., 2014). This was achieved by a preliminary drought experiment on five individuals for each species. These individuals were located in the greenhouse with no water addition, and every 1 to 3 days, the Ψ_{PD} and Ψ_{MD} of three randomly chosen individuals were measured. After removal of measurements with Ψ_{PD} near 0 (0%–20% of data), the Ψ_{MD} was regressed against Ψ_{PD}, and the slope (σ) and intercept (Λ) were estimated (Martínez-Vilalta et al., 2014).

Physiological and biomass measurements

During the drought period, spot measurements of leaf water potentials, photosynthesis, transpiration, stomatal conductance, leaf area, and plant biomass were conducted every 3–5 days. These variables were measured every 1–2 days at the beginning but every 3–7 days during the late phase of the rewatering period. For each measurement point during the drought and rewatering periods, Ψ_{PD} (2:00–4:00 a.m.) and Ψ_{MD} (12:00–14:00 p.m.) were measured on three leaves (one per individual) for each species ($n = 3$). For plants that became partially defoliated, we chose leaves that had no obvious sign of wilting to determine Ψ_{PD} and Ψ_{MD}. Ψ_{MD} was affected not only by the soil water potential (SWP) but also by transpiration rate at the time of collection. To avoid the uncertainty induced by different weather conditions on different days, we used the Ψ_{PD} measurements to calculate stem PLC during the drought period based on the predetermined vulnerability curves. Although it was uncertain whether the vulnerability

curves differed between drought and rewatering periods (Duan et al., 2019), Hudson et al. (2018) found no response of vulnerability curve to water treatments in piñons and junipers. Therefore, we also calculated the stem PLC during the recovery period based on the vulnerability curves collected. After measurements of leaf water status, the plants were destructively sampled and separated into leaves, stems, and roots. All the leaves were scanned, and the total leaf area was determined by ImageJ (version 1.51s) software. All the samples were oven-dried, and the biomass of leaves, stems, and roots was measured. Net photosynthesis (A), transpiration (E), and stomatal conductance (g_s) were measured on three nondestructive individuals for each species and each treatment using LI-6400 during the 8:00–11:00 a.m. period. The temperature, relative humidity, and light intensity were maintained around 25°C, 60%, and 1000 μ mol m^{-2} s^{-1}, respectively. The CO_2 concentration was set to ambient. To better illustrate the result, A, E, and g_s in drought–rewatering groups were normalized by dividing them by the values of the control group.

Drought resistance and recovery

To quantify how A and E respond to drought, we adopted the framework in Hodgson et al. (2015), which used state change (SC) and return time (RT) to quantify the ability of a system to resist and recover from disturbance. For a specific day, the SC was $(1 - y_{norm}) \times 100\%$, where y_{norm} is the normalized A or E. The smaller the SC, the higher the resistance. For each recovery trajectory, y_{norm} was fitted against the days after rewatering (DAR) by an empirical equation as follows:

$$y_{norm} = a_1 + a_2 \times \frac{DAR^{a_3}}{DAR^{a_3} + a_4}, \quad (7)$$

where a_1 represents the y_{norm} before rewatering, $(a_1 + a_2)$ determines the maximum extent that A or E could recover to, and a_3 is a shape parameter accounting for the variation in the shape of recovery trajectory among species. Based on Equation (7), the RT to x percentage (RT_x) is

$$RT_x = \sqrt[a_3]{\frac{a_4(x\% - a_1)}{a_1 + a_2 - x\%}}. \quad (8)$$

We used $x = 20$, 50, and 80 to indicate the A and E recovery to low, medium, and high levels, respectively. The smaller the RT_x, the faster the recovery. To avoid overparameterization in Equation (6), linear interpolation was applied to calculate the RT if A or E recovered very quickly and exhibited a linear trajectory. The lower limit of RT was set to 0.5 because we rewatered the plants in the evening.

We also determined the survival time under drought according to the physiological measurements and rewatering experiments. The maximum survival time was defined as the drought days with all the leaves being brown or defoliated or no recovery was observed after rewatering. The minimum survival time was defined as the longest drought days after which at least 50% of leaves were green. The average survival time was calculated as the mean of the minimum and maximum.

Statistics

Differences in plant traits among five species were tested by one-way ANOVA or Kruskall–Wallis test. The regulation of plant traits on mortality, resistance, and recovery were investigated by regressing the survival time, SC, and RT against traits. The normality and homogeneity assumptions were checked by both plotting (Q-Q plot and scatter plot of model residuals for normality and homogeneity assumptions, respectively) and statistical methods (Shapiro–Wilk test and Fligner–Killeen test, respectively). For ANOVA, the traits clearly violating normality or homogeneity assumptions (root: shoot ratio, SLA, LDMC, LA:BA, π_{tlp}, and ε) were analyzed by Kruskall–Wallis tests. For the traits derived from curve fitting that did not have real replications (P_{50}, P_{88}, Ψ_{close}, $HSM_{close\text{-}88}$, $HSM_{min\text{-}88}$), we used ANOVA from sufficient statistics for groups to conduct multiple comparisons among species (the aov.sufficient function in the HH R package). For regressions, no clear violation of normality or homogeneity assumptions were found. All analyses were applied in R version 3.5.1 (R Core Team, 2018).

RESULTS

Environmental variables and extent of hydraulic failure

During the drought–rewatering experiment, the mean air temperature and relative humidity in the greenhouse were 32.1 ± 3.0°C and 71.6 ± 7.2% (mean ± SD), respectively (Figure 2a). The SWC in the control treatment was maintained at 21.1 ± 2.4% (Figure 2b). The SWC in drought–rewatering treatments showed similar patterns among the five species. During the drought period, the SWC dropped to ~5% after 20 days of withholding water.

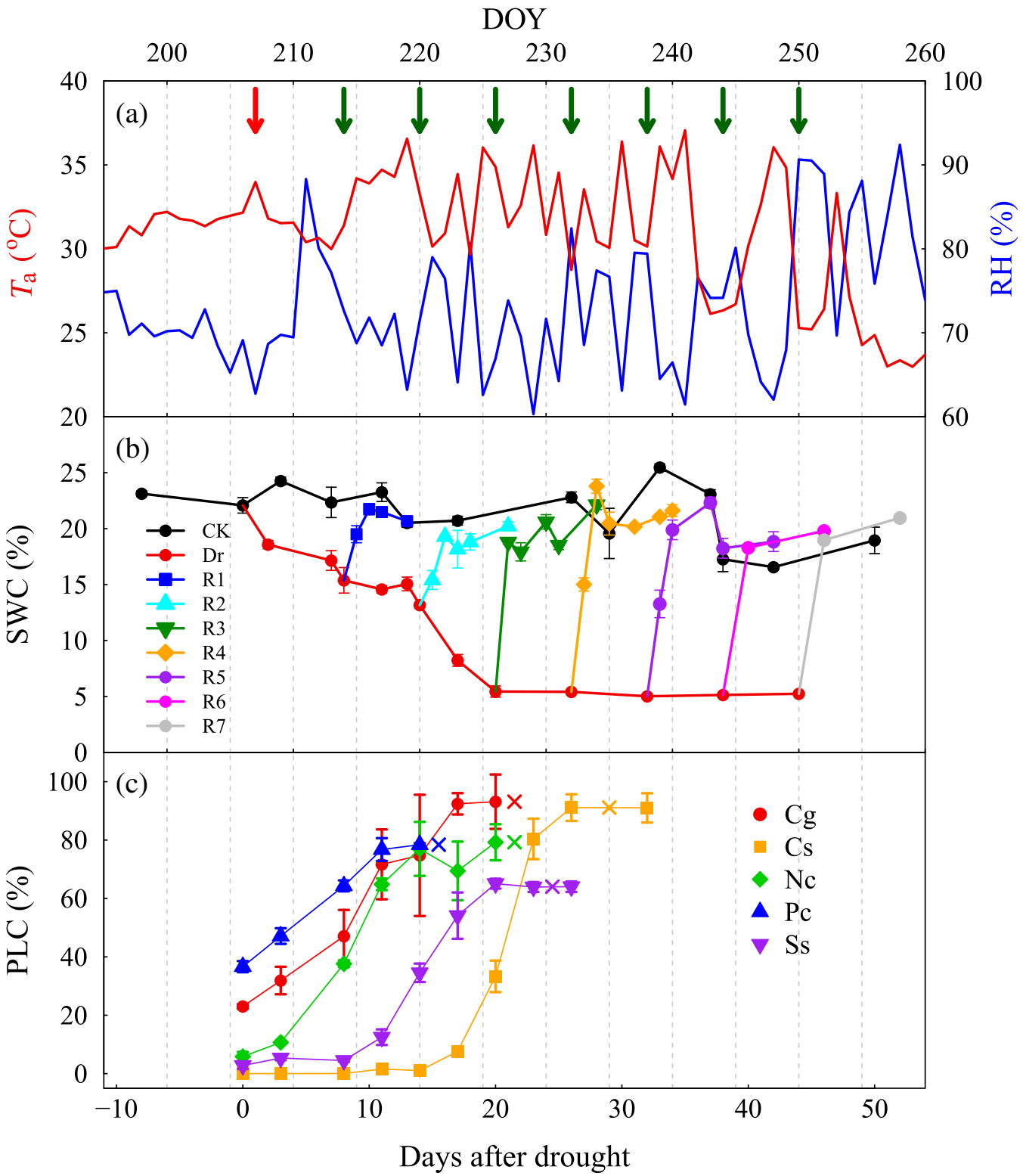

FIGURE 2 Dynamics in air temperature (T_a), relative humidity (RH), soil water content (SWC), and PLC during the experiments. The red and green arrows in (a) indicate the onsets of drought and rewetting treatments, respectively. The colored crosses in (c) represent the average survival days of each species. DOY, day of year; CK, control; Dr, drought treatment; R1–R7, rewetting after 8, 14, 20, 26, 32, 38, and 44 days' drought, respectively. Cg, *Cyclobalanopsis gilva*; Cs, *Castanopsis sclerophylla*; Nc, *Neocinnamomum chekiangense*; Pc, *Phoebe chekiangensis*; Ss, *Schima superba*.

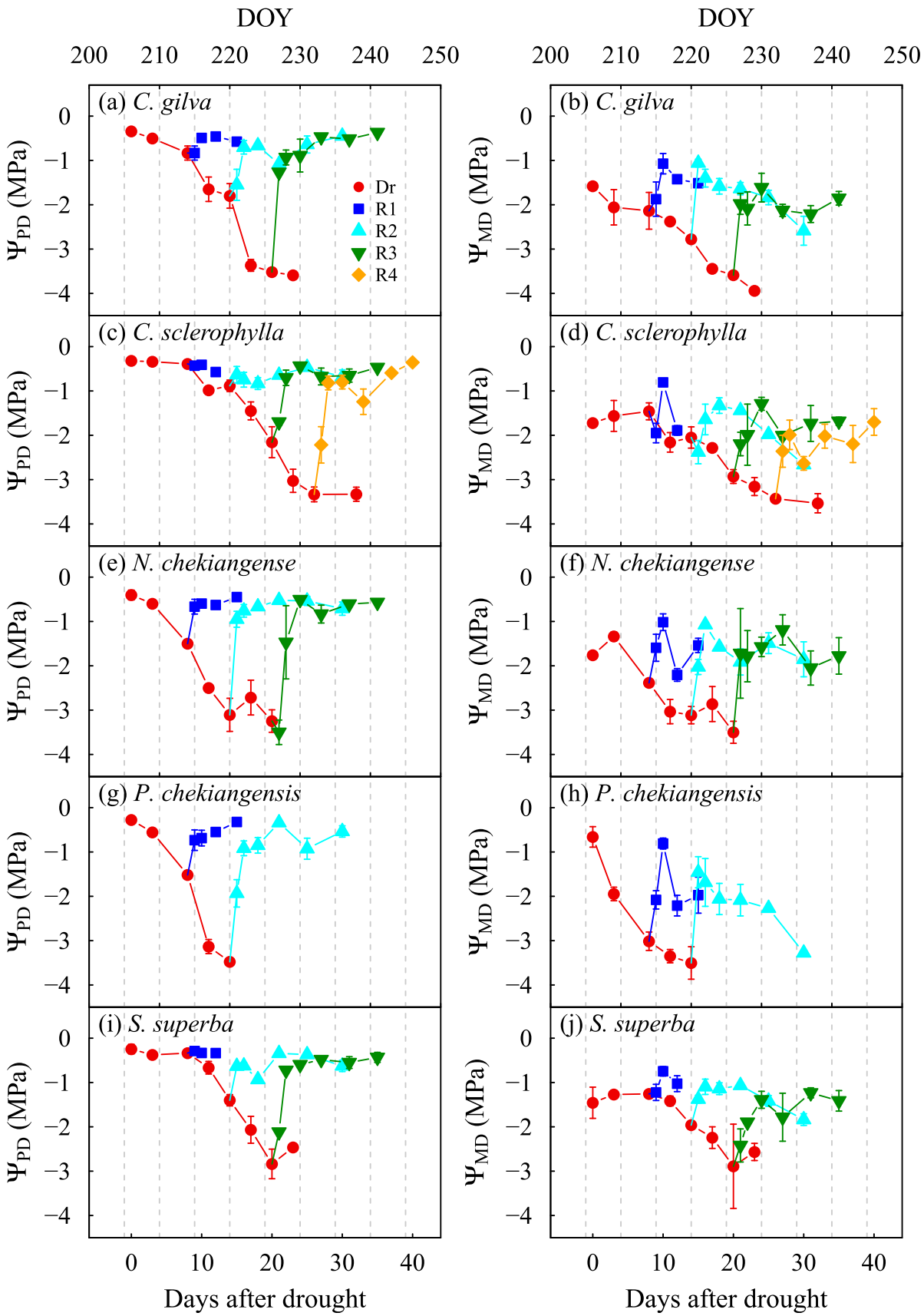

FIGURE 3 The response and recovery of (a, c, e, g, i) predawn and (b, d, f, h, j) midday leaf water potentials to persistent drought and rewetting for the five species. DOY, day of year; Dr, drought treatment; R1, rewetting after 8 days' drought; R2, rewetting after 14 days' drought; R3, rewetting after 20 days' drought; R4, rewetting after 26 days' drought.

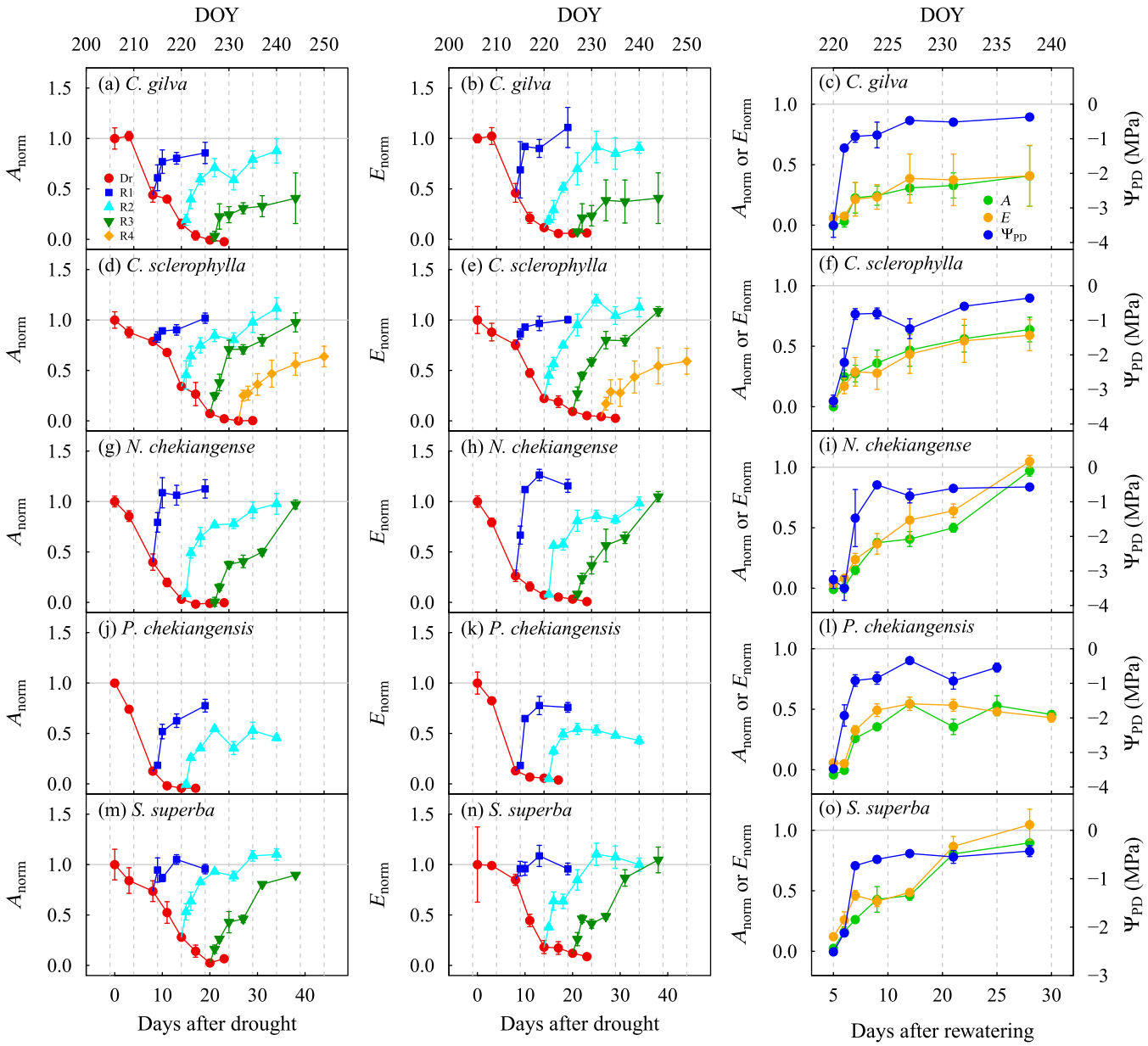

FIGURE 4 Response and recovery of (a, d, g, j, m) *A*, photosynthesis rate and (b, e, h, k, n) *E*, transpiration rate to persistent drought and rewetting, and (c, f, i, l, o) comparisons of the recovery of leaf water potential, *A* and *E*. Note that the *A* and *E* were normalized for the convenience of comparisons. The third column shows recovery from the most severe drought before tree death. The gray horizontal lines represent the A_{norm} and E_{norm} of plants in CK groups. DOY, day of year; Dr, drought treatment; R1, rewetting after 8 days' drought; R2, rewetting after 14 days' drought; R3, rewetting after 20 days' drought; R4, rewetting after 26 days' drought.

During the rewatering period, the SWC rapidly recovered to the control levels within 2 days (Figure 2b).

During the drought period, the extent of stem hydraulic failure, indicated by PLC, increased with soil drying (Figure 2c). After the same duration of drought, the stem PLC of *C. sclerophylla* and *S. superba* was lower than that of the other species. Specifically, the lethal PLC threshold was 93%, 91%, 79%, 78%, and 64% for *C. gilva*, *C. sclerophylla*, *N. chekiangense*, *P. chekiangensis*, and *S. superba*, respectively ($F_{4,10} = 4.461$, $p = 0.025$, Figure 2c).

Difference in plant traits among species

Morphologically, there were differences among the five species. Plant height and basal diameter were largest in *N. chekiangense*, whereas leaf size was largest in *P. chekiangensis* (Table 1). Differences in SLA, LDMC, and wood density were small (Table 1). No significant difference was found in root:shoot, leaf area:basal area ratio, or photosynthetic traits (Table 1).

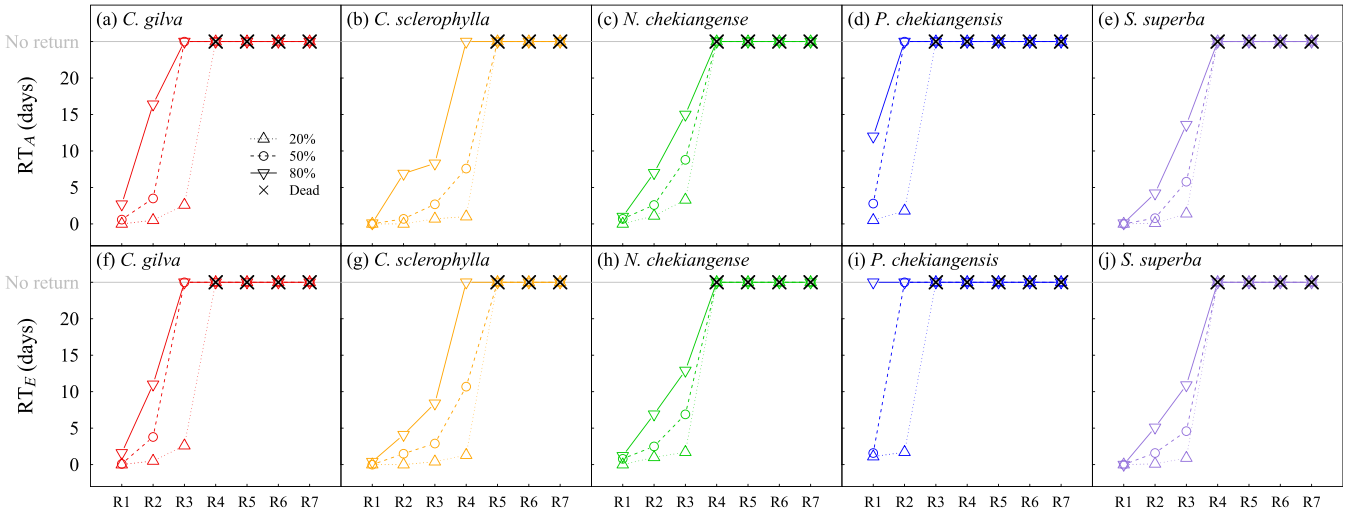

FIGURE 5 The 20%, 50%, and 80% return time (RT) of (a–e) photosynthesis and (f–j) transpiration in five species during rewatering period. The shorter the RT, the higher the resilience. The horizontal gray line indicates the plant is not able to return to the specific percentage of control. The red, orange, green, blue and purple symbols represent *C. gilva*, *C. sclerophylla*, *N. chekiangense*, *P. chekiangensis* and *S. superba*, respectively. The black crosses indicate plant death. R1, rewetting after 8 days' drought; R2, rewetting after 14 days' drought; R3, rewetting after 20 days' drought; R4, rewetting after 26 days' drought.

For the hydraulic traits, *C. sclerophylla* and *S. superba* were more resistant to embolism (i.e., more negative stem water potential causing 50% PLC, P_{50}), whereas *N. chekiangense* and *P. chekiangensis* were more drought tolerant with more negative turgor loss point (π_{tlp}) and larger modulus of elasticity (ε) (Table 1). However, the degree of anisohydricity (σ) was not significantly different among species (Table 1).

Ninety percent stomatal closure occurred later in *C. sclerophylla* and *S. superba* than in other species (Table 1; Appendix S1: Figure S1). The HSM, calculated as the difference between the minimum leaf water potential and P_{88} ($HSM_{min\text{-}88}$), was largest in *P. chekiangensis*, followed by *S. superba*, *C. sclerophylla*, *N. chekiangense*, and *C. gilva* (Table 1). The $HSM_{close\text{-}88}$, calculated as the difference between Ψ_{close} and P_{88}, was also largest in *P. chekiangensis* but lowest in *N. chekiangense* (Table 1).

Tree physiology and mortality under drought and rewatering periods

During the drought period, severe defoliation (>50%) occurred after 14, 20, 20, 26, and 32 days of drought for *P. chekiangensis*, *C. gilva*, *N. chekiangense*, *S. superba*, and *C. sclerophylla*, respectively (Appendix S1: Figure S2). During the rewatering period, no new leaves developed in the defoliated plants. Both predawn (Ψ_{PD}) and midday leaf water potentials (Ψ_{MD}) decreased gradually during drought and recovered to the predrought levels within 3 days after rewatering if there was no severe defoliation (Figure 3). The recovery pattern of stem PLC was similar to that of leaf water potential (Appendix S1: Figure S3).

The response and recovery patterns were similar among *A*, *E*, and g_s (Figure 4; Appendix S1: Figure S3). These variables could not fully recover when the drought ended after 8, 20, 26, 26, and 26 days for *P. chekiangensis*, *C. gilva*, *N. chekiangense*, *S. superba*, and *C. sclerophylla*, respectively. The recovery velocity of *A* and *E* was much lower than those of SWC and leaf water status, especially under conditions of severe droughts (Figure 4c,f,i,l,o). For *C. gilva*, *C. sclerophylla*, and *P. chekiangensis*, the leaf potential recovered to predrought level under severe drought but the *A* and *E* only exhibited partial recovery (Figure 4).

The resistance (indicated by the SC) and recovery (indicated by the RT) of *A* and *E* differed among species and drought intensities (Appendix S1: Figure S4). During the drought period, *P. chekiangensis* was the least resistant species, with the largest SC of both *A* and *E*, followed by *N. chekiangense*, *C. gilva*, *S. superba*, and *C. sclerophylla*. Although the SC of *E* in *S. superba* was similar to that in *C. sclerophylla*, *S. superba* defoliated and died before *C. sclerophylla* (Appendix S1: Figures S2 and S5).

P. chekiangensis was also the species that recovered slowest from drought, whose RT_{80} (RT to 80% of the control value) was much higher than other species in the R1 treatment (rewatering after 8 days of drought) and died after 20 days of drought (Figure 5d,i). *N. chekiangense* and *C. gilva* both died after 26 days of drought

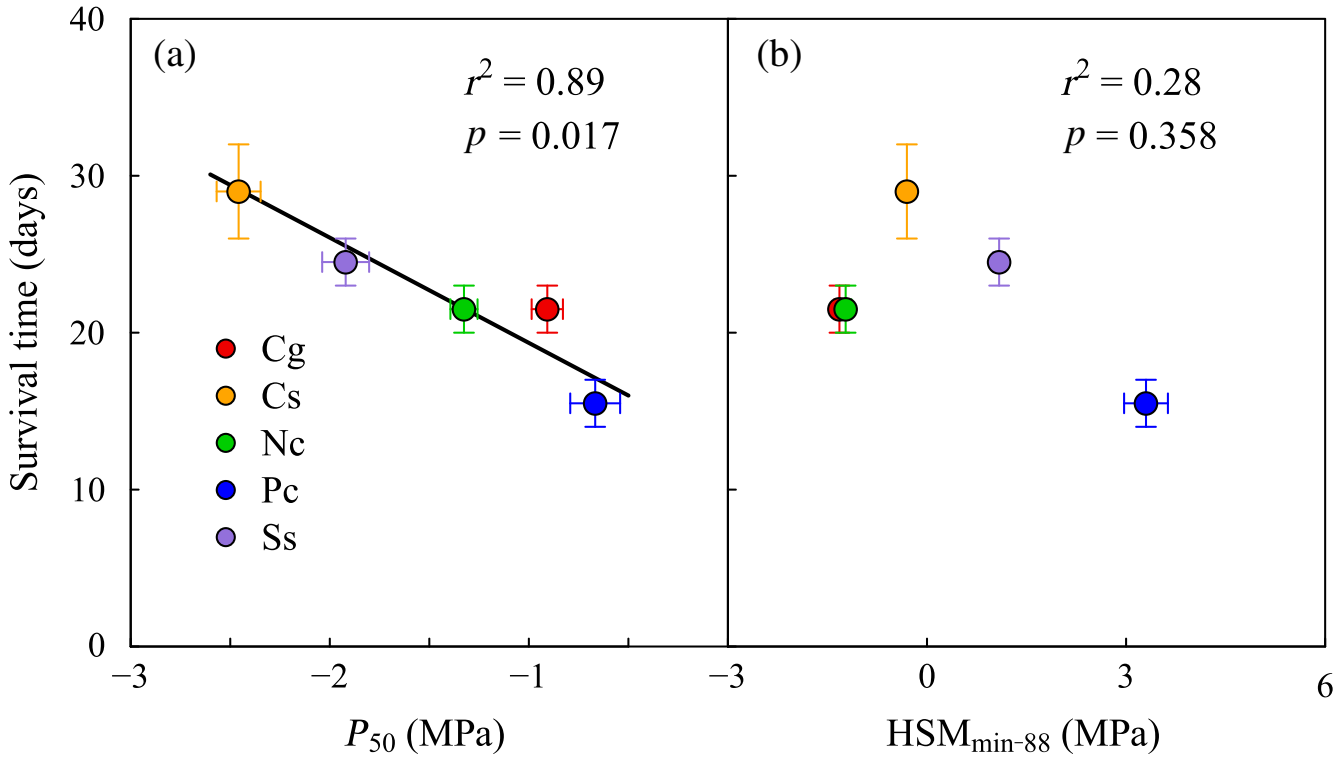

FIGURE 6 Influences of P_{50} and HSM_{min-88} on survival time. Cg, *Cyclobalanopsis gilva*; Cs, *Castanopsis sclerophylla*; Nc, *Neocinnamomum chekiangense*; Pc, *Phoebe chekiangensis*; Ss, *Schima superba*.

(Figure 5a,c,f,h). However, *C. gilva* had longer RT_{80} than *N. chekiangense* in R2 treatment (rewatering after 14 days of drought) and could not recover to 50% of the control value in the R3 treatment (rewatering after 20 days of drought). *S. superba* also died after 26 days of drought, but its RTs were slightly lower than *N. chekiangense*'s (Figure 5e,j). *C. sclerophylla* was the most resilient species, which could recover to 50% of the control value in the R4 treatment (rewatering after 26 days of drought) and did not die until 32 days of drought (Figure 5b,g).

Relationships between plant traits and tree resistance, recovery, and mortality

Among all the morphological, photosynthetic, and hydraulic traits, only the stem embolism resistance (P_{50}) could explain the variance in tree mortality, resistance, and recovery among five species. The species that survived more days during drought had more negative P_{50} values ($r^2 = 0.89$, $p = 0.017$, Figure 6a). With decreasing P_{50}, both the SC and RT decreased. The influence of stem P_{50} was alleviated for resistance but enhanced for recovery when the drought intensity increased (Figure 7). Neither HSM_{min-88} nor $HSM_{close-88}$ could explain the interspecific differences in tree mortality, SC, or RT (Figure 6b; Appendix S1: Figures S6 and S7). In addition, no significant relationship was found between stem P_{50} and other traits (Appendix S1: Table S1).

DISCUSSION

Regulation of embolism resistance on tree mortality

In this study, species with greater stem embolism resistance (more negative P_{50}) survived longer under persistent drought (Figure 6a), reflecting the important role of hydraulic failure in tree mortality. Some studies interpreted the influence of stem embolism resistance on tree death as the risk that trees would reach the lethal hydraulic failure (e.g., 88% PLC), which was usually indicated by the HSM (Anderegg et al., 2016). However, we found that neither HSM_{min-88} nor $HSM_{close-88}$ was correlated to the survival time or drought resilience among the five species (Figure 6b; Appendix S1: Figures S5–S7). This might have been due to the lack of a general stem PLC threshold for tree death. For example, Adams et al. (2017) and McDowell et al. (2013) suggested that the lethal stem

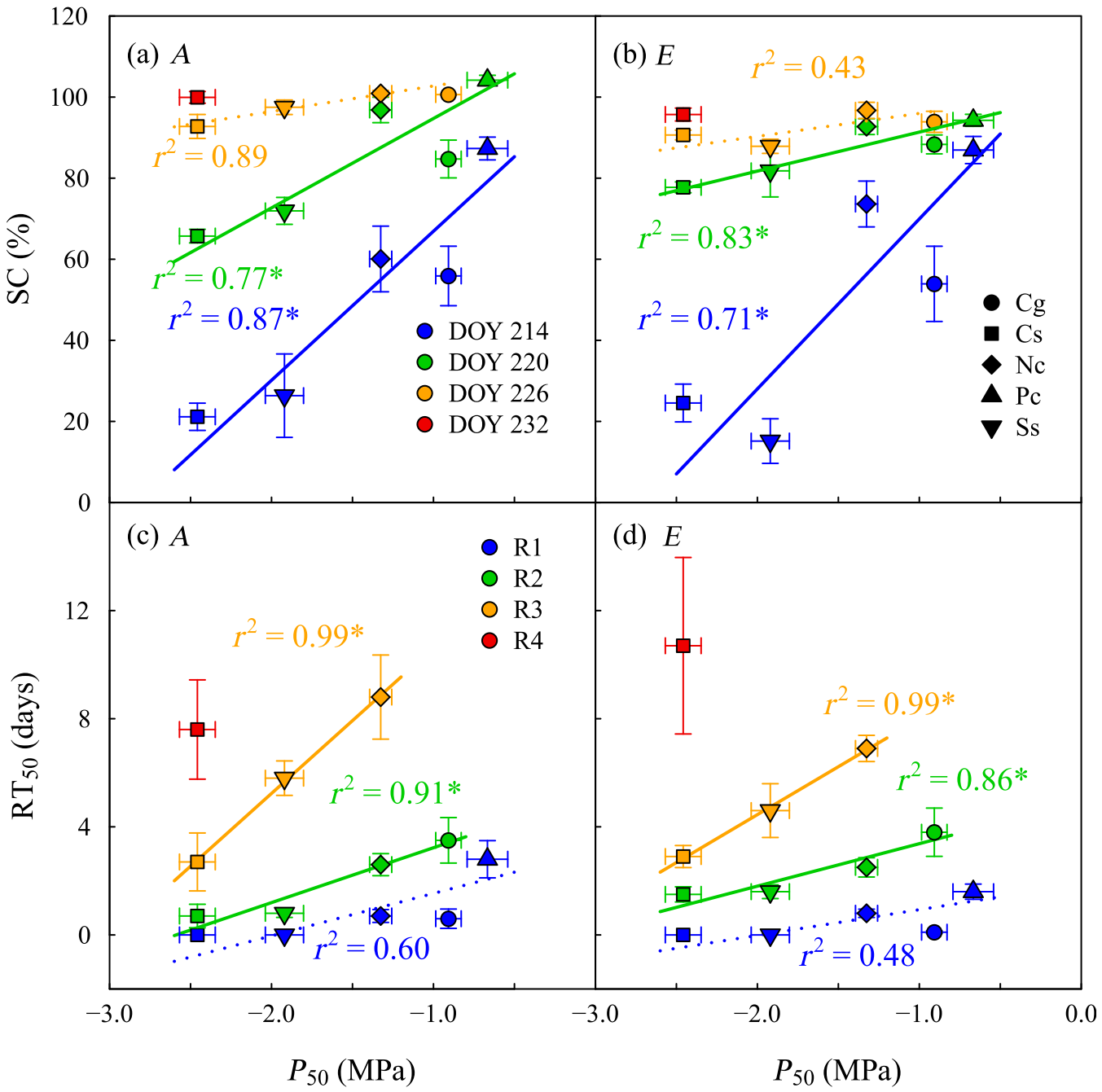

FIGURE 7 Influences of P_{50} on resistance (indicated by the SC) and recovery (indicated by 50% return time, RT_{50}) of (*A*) photosynthesis and (*E*) transpiration to persistent drought and rewatering, respectively. The SC was the values at DOY 214, 220, 226, and 232, respectively. DOY, day of year. Cg, *Cyclobalanopsis gilva*; Cs, *Castanopsis sclerophylla*; Nc, *Neocinnamomum chekiangense*; Pc, *Phoebe chekiangensis*; Ss, *Schima superba*. R1, rewetting after 8 days' drought; R2, rewetting after 14 days' drought; R3, rewetting after 20 days' drought; R4, rewetting after 26 days' drought.

PLC exceeded 60%, whereas Li, McCormack, et al. (2015) showed that this value could be as high as 100%. In our study, the stem PLC threshold causing death varied from 64% to 93% (Figure 2c). The observed lethal stem PLC might also be related to drought intensity and duration. In our experiment, the drought was rapid and severe, having a direct impact on the stem hydraulics. If a more gradual and longer duration drought was conducted, the lethal stem PLC might be smaller than our observation in two situations: (1) the xylem embolism continuously develops even after the relief of drought stress (Gauthey et al., 2022) or (2) the persistent drought depletes the nonstructural carbohydrates, which is important to signaling of stomatal response, osmotic adjustments, and embolism refilling (Klein et al., 2018; Pou et al., 2012).

Previous studies also showed other traits, such as anisohydricity and turgor loss point, could be important to tree death or drought resistance (Bartlett et al., 2016; Kannenberg et al., 2019). For instance, Martin-StPaul et al. (2017) showed that 90% stomatal closure generally occurred before 50% stem PLC, avoiding further water loss under drought. However, our results showed the opposite pattern (except for *C. sclerophylla*, Appendix S1: Figure S1a). In this study, the more drought-resistant species closed stomata later than the less-resistant ones (Appendix S1: Figure S1b). This evidence suggested that the reduced water loss due to stomatal closure might not be the primary factor causing the different drought resistance and mortality among the five species. Similarly, although leaf shedding may reduce water loss (Xu et al., 2010), the species with earlier defoliation (*C. gilva*, *N. chekiangense*, and *P. chekiangensis*) did not have higher drought resilience (Appendix S1: Figures S1 and S2).

Turgor loss point (π_{tlp}) is another key trait that might be correlated with embolism resistance and tree mortality (Bartlett et al., 2016; Zhu et al., 2018). However, in this study, species with more negative π_{tlp} (*P. chekiangensis* and *N. chekiangense*) did not show higher drought resistance or longer survival time, instead of being highly sensitive to soil drying. Consistent with our results, another drought–rewatering experiment on three SEBF species in southern China suggested that the most drought-resistant species had the highest embolism resistance but not the largest π_{tlp} (Duan et al., 2019). More broadly, a global meta-analysis also showed a nonsignificant effect of π_{tlp} on tree mortality (Anderegg et al., 2016). All these pieces of evidence suggest that the differential P_{50} among five species may actually reflect a passive response to drought, not active mechanism coping with drought stress.

Regulation of embolism resistance in drought recovery of *A* and *E*

Previous studies suggested that plant hydraulic traits, such as embolism resistance and isohydricity, may regulate the recovery of physiological rates (Brodribb et al., 2010; Peguero-Pina et al., 2018; Pou et al., 2012). In our study, however, only the stem embolism resistance had significant effects on the recovery time of photosynthesis and transpiration among five species (Figures 7c,d), highlighting the importance of hydraulic dysfunction in limiting the postdrought recovery (Peguero-Pina et al., 2018; Urli et al., 2013). The recovery of hydraulic function can be achieved via two mechanisms: embolism refilling and new xylem growth (Klein et al., 2018). Embolism refilling occurs in very short time spans (6–12 h) (Gauthey et al., 2022), which might be important under mild and short droughts. When plants experience more severe drought, the xylem conduits might be damaged permanently. Thus, the recovery of plant water potential largely depends on the growth of new xylem, a process taking from weeks to months (Brodribb et al., 2010; Duan et al., 2019). In our study, the leaf water potential and apparent stem PLC recovered within 2–3 days after rewatering as long as there was no severe defoliation (Figure 2; Appendix S1: Figure S3), indicating that the rapid refilling might repair the xylem embolism. However, a recent study using micro–computed tomography to examine the xylem embolism in *Eucalyptus saligna* suggested that the stem water potential could fully recover in 24 h despite the absence of embolism refilling or new xylem growth (Gauthey et al., 2022), suggesting further research is required to explicitly resolve the debate on the mechanisms underlying the postdrought recovery of plant water status.

The recovery of photosynthesis and transpiration largely lagged behind that of leaf water status, taking 1–3 weeks to reach normal levels (Figure 4), probably due to the delayed recovery of stomatal conductance and biochemical components of photosynthesis (Li et al., 2021). The reduction of stomatal conductance under drought can be induced not only by hydraulic factors but also by nonhydraulic factors, such as abscisic acid (ABA; Flexas et al., 2009; Creek et al., 2018). After rewatering, when the hydraulic system recovers, the previously accumulated ABA may still limit stomatal conductance (McAdam & Brodribb, 2015), causing a slow recovery of photosynthesis and transpiration. The biochemical components (e.g., V_{cmax} and J_{max}) could be decreased by severe drought due to the inactivation of photosynthetic enzymes, thereby limiting the recovery rate of photosynthesis (Flexas et al., 2009; Li et al., 2021). In addition, drought-induced cell destruction may also delay the recovery of stomatal conductance (Miyashita et al., 2005) and even cause permanent damage to the photosynthetic system (Trueba et al., 2019), leading to incomplete recovery in tree physiology under severe droughts (Figure 4).

Implications

SEBFs in China are unique biomes with high biodiversity and carbon sequestration (Fan et al., 2018; Yu et al., 2014) and experiences more frequent extreme droughts (Yuan et al., 2016). It is difficult to directly apply our seedling results to mature trees (Hartmann et al., 2018). However, the inferences on seedlings could still be valuable for the potential vulnerability of SEBFs because forest restoration after destructive disturbances, such as extreme droughts and typhoon (Lin et al., 2011),

depends on the regeneration of tree seedlings. In this study, the slight contribution of stomatal closure, leaf shedding, and drought tolerance to drought resilience in SEBF seedlings may be derived from the evolutionary background of these trees. Because the SEBFs have historically suffered internal drought rarely in their evolutionary history, they may not have developed multiple drought strategies to increase their fitness. As a result, the SEBFs might be vulnerable to future co-occurring climate extremes due to the failure of species regeneration. In fact, the difficulty of species regeneration caused by natural and human disturbances has already threatened the maintenance of SEBFs in southern China (Chu et al., 2019; Liu et al., 2018).

At the ecosystem scale, the forests in South America, Africa, and Southeast Asia were more isohydric (i.e., rapid stomatal closure under drought) than SEBFs (Konings & Gentine, 2017), suggesting a more effective drought strategy of these forests. Thus, SEBFs might be more vulnerable to future drought than the forests in these areas, probably because SEBFs have experienced less drought stress. Bennett et al. (2021) also suggested that more severe historical drought stresses made the African tropical forests more drought-adapted and more resistant to El Niño-induced droughts than Amazonian and Southeast Asian forests. This conclusion was consistent with the observation that tree mortality rate greatly increased in Amazon forests but slightly decreased in the Congo Basin (McDowell et al., 2022). However, contrary evidence exists. Zhu et al. (2019) argued that SEBFs had less risk of hydraulic failure than tropical dry forests and Mediterranean-type woodlands because of the wider HSMs. As we discussed, HSM might not be a reliable indicator of drought vulnerability for SEBFs. Nevertheless, considering the scarcity of studies that directly examine drought mortality and recovery in SEBFs, more drought–rewatering experiments are needed to investigate the actual vulnerability of SEBFs to future drought.

There were some uncertainties worth highlighting that might provide insight for the future researchers. First, our drought treatment was very rapid and severe, which could be different from naturally occurring drought. If trees are subject to more gradual and mild droughts, the stem hydraulic failure might occur more slowly, allowing other physiological processes (e.g., stomatal closure, leaf shedding, and osmotic adjustments) to take part in the process of tree death. In this case, other hydraulic traits could be related to drought resistance and resilience. Second, when the SWC is low, the SWP could change dramatically, even when the SWC remains relatively unchanged. Therefore, tracking the SWP during an experiment could help to better understand the exact external drought stresses that plants experience. Third, studies involving repeated drought events showed that early exposure to water deficit could induce physiological or morphological changes that improved plant performance under later extreme droughts (Wang et al., 2017). Studies on multiple ecotypes or genotypes within the same species showed that the plasticity of physiological rates and hydraulic traits to drought could be adaptive (Challis et al., 2022; Duan et al., 2022). The existence of physiological acclimation and adaptation might help SEBFs to buffer the damage caused by severe droughts. All these issues reflect the complex mechanisms underlying drought response and recovery, which should be further studied to address the challenge of incorporating hydraulic dynamics into terrestrial biosphere models to better predict forest carbon and water cycling under future climate change (Medlyn et al., 2016).

AUTHOR CONTRIBUTIONS

Junjiong Shao and Xuhui Zhou conceived the study. Junjiong Shao, Peipei Zhang, Deping Zhai, Tengfei Yuan, and Zhen Li conducted the experiments. Junjiong Shao analyzed the data. Junjiong Shao and Xuhui Zhou led the writing with contributions from all authors.

ACKNOWLEDGMENTS

The authors thank the editor and two anonymous reviewers for their insightful comments and suggestions. This study was financially supported by the National Natural Science Foundation of China (Grants 31930072 and 31600387) and the National Key Research and Development Program of China (2017YFA06046). NGM was supported by the Department of Energy's Next Generation Ecosystem Experiment (NGEE)-Tropics project. We thank Weisong Cheng, Jing Gao, Nan Li, Ruiqiang Liu, Qin Luo, Jiawei Wang, Qing Wang, Guodong Zhang, Huimin Zhou, and Guiyao Zhou for their great help to the experiment.

CONFLICT OF INTEREST

The authors declare no conflict of interest.

DATA AVAILABILITY STATEMENT

Data (Shao, 2022) is archived in Figshare at https://doi.org/10.6084/m9.figshare.20326380.v1.

ORCID

Xuhui Zhou https://orcid.org/0000-0002-2038-9901
Nate G. McDowell https://orcid.org/0000-0002-2178-2254

REFERENCES

Adams, H. D., M. J. B. Zeppel, W. R. L. Anderegg, H. Hartmann, S. M. Landhäusser, D. T. Tissue, T. E. Huxman, et al. 2017. "A Multi-Species Synthesis of Physiological Mechanisms in Drought-Induced Tree Mortality." *Nature Ecology and Evolution* 1: 1285–91.

Anderegg, W. R. L., T. Klein, M. Bartlett, L. Sack, A. F. A. Pellegrini, B. Choat, and S. Jansen. 2016. "Meta-Analysis Reveals that Hydraulic Traits Explain Cross-Species Patterns of Drought-Induced Tree Mortality across the Globe." *Proceedings of the National Academy of Sciences* 113: 5024–9.

Bartlett, M. K., T. Klein, S. Jansen, B. Choat, and L. Sack. 2016. "The Correlations and Sequence of Plant Stomatal, Hydraulic, and Wilting Responses to Drought." *Proceedings of the National Academy of Sciences* 113: 13098–103.

Bennett, A. C., G. C. Dargie, A. Cuni-Sanchez, J. T. Mukendi, W. Hubau, J. M. Mukinzi, O. L. Phillips, et al. 2021. "Resistance of African Tropical Forests to an Extreme Climate Anomaly." *Proceedings of the National Academy of Sciences* 118: e2003169118.

Brodribb, T. J., D. J. M. S. Bowman, S. Nichols, S. Delzon, and R. Burlett. 2010. "Xylem Function and Growth Rate Interact to Determine Recovery Rates after Exposure to Extreme Water Deficit." *New Phytologist* 188: 533–42.

Challis, A., C. Blackman, C. Ahrens, B. Medlyn, P. Rymer, and D. Tissue. 2022. "Adaptive Plasticity in Plant Traits Increases Time to Hydraulic Failure under Drought in a Foundation Tree." *Tree Physiology* 42: 708–21.

Chu, X., X. Wang, D. Zhang, X. Wu, and Z. Zhou. 2019. "Responses of *Taxus chinensis* and *Phoebe chekiangensis* Seedlings to Controlled-Release Fertilizer in Various Formulations and Application Rates." *iForest - Biogeosciences and Forestry* 12: 254–61.

Creek, D., C. J. Blackman, T. J. Brodribb, B. Choat, and D. T. Tissue. 2018. "Coordination between Leaf, Stem, and Root Hydraulics and Gas Exchange in Three Arid-Zone Angiosperms during Severe Drought and Recovery: Coordination between Hydraulics and Gas Exchange during Drought and Recovery." *Plant, Cell & Environment* 41: 2869–81.

Dai, A. 2013. "Increasing Drought under Global Warming in Observations and Models." *Nature Climate Change* 3: 52–8.

de A. Lobo, F., M. P. de Barros, H. J. Dalmagro, Â. C. Dalmolin, W. E. Pereira, É. C. de Souza, G. L. Vourlitis, and C. E. Rodríguez Ortíz. 2013. "Fitting Net Photosynthetic Light-Response Curves with Microsoft Excel—A Critical Look at the Models." *Photosynthetica* 51: 445–56.

Duan, H., V. R. de Dios, D. Wang, N. Zhao, G. Huang, W. Liu, J. Wu, S. Zhou, B. Choat, and D. T. Tissue. 2022. "Testing the Limits of Plant Drought Stress and Subsequent Recovery in Four Provenances of a Widely Distributed Subtropical Tree Species." *Pllant, Cell and Environment* 45: 1187–203.

Duan, H., Y. Li, Y. Xu, S. Zhou, J. Liu, D. T. Tissue, and J. Liu. 2019. "Contrasting Drought Sensitivity and Post-Drought Resilience among Three co-Occurring Tree Species in Subtropical China." *Agricultural and Forest Meteorology* 272–273: 55–68.

Duursma, R. A. 2015. "Plantecophys - an R Package for Analysing and Modelling Leaf Gas Exchange Data." *PLoS One* 10: e0143346.

Fan, D., J. Huang, H. Hu, Z. Sun, S. Cheng, Y. Kou, and Z. Zhang. 2018. "Evolutionary Hotspots of Seed Plants in Subtropical China: A Comparison with Species Diversity Hotspots of Woody Seed Plants." *Frontiers in Genetics* 9: 333.

Flexas, J., M. Barón, J. Bota, J.-M. Ducruet, A. Gallé, J. Galmés, M. Jiménez, et al. 2009. "Photosynthesis Limitations during Water Stress Acclimation and Recovery in the Drought-Adapted *Vitis* Hybrid Richter-110 (*V. berlandierix* × *V. rupestris*)." *Journal of Experimental Botany* 60: 2361–77.

Garcia-Forner, N., H. D. Adams, S. Sevanto, A. D. Collins, L. T. Dickman, P. J. Hudson, M. J. B. Zeppel, et al. 2016. "Responses of Two Semiarid Conifer Tree Species to Reduced Precipitation and Warming Reveal New Perspectives for Stomatal Regulation." *Plant, Cell and Environment* 39: 38–49.

Gauthey, A., J. M. R. Peters, R. Lòpez, M. R. Carins-Murphy, C. M. Rodriguez-Dominguez, D. T. Tissue, B. E. Medlyn, T. J. Brodribb, and B. Choat. 2022. "Mechanisms of Xylem Hydraulic Recovery after Drought in *Eucalyptus saligna*." *Plant, Cell and Environment* 45: 1216–28.

Hammond, W. M., K. Yu, L. A. Wilson, R. E. Will, W. R. L. Anderegg, and H. D. Adams. 2019. "Dead or Dying? Quantifying the Point of no Return from Hydraulic Failure in Drought-Induced Tree Mortality." *New Phytologist* 223: 1834–43.

Hartmann, H., C. F. Moura, W. R. L. Anderegg, N. K. Ruehr, Y. Salmon, C. D. Allen, S. K. Arndt, et al. 2018. "Research Frontiers for Improving our Understanding of Drought-Induced Tree and Forest Mortality." *New Phytologist* 218: 15–28.

Haughton, N., G. Abramowitz, M. G. De Kauwe, and A. J. Pitman. 2018. "Does Predictability of Fluxes Vary between FLUXNET Sites?" *Biogeosciences* 15: 4495–513.

Hodgson, D., J. L. McDonald, and D. J. Hosken. 2015. "What Do you Mean, "Resilient"?" *Trends in Ecology and Evolution* 30: 503–6.

Hudson, P. J., J. M. Limousin, D. J. Krofcheck, A. L. Boutz, R. E. Pangle, N. Gehres, N. G. McDowell, and W. T. Pockman. 2018. "Impacts of Long-Term Precipitation Manipulation on Hydraulic Architecture and Xylem Anatomy of piñon and Juniper in Southwest USA." *Plant, Cell and Environment* 41: 421–35.

Jacobsen, A. L., R. B. Pratt, M. F. Tobin, U. G. Hacke, and F. W. Ewers. 2012. "A Global Analysis of Xylem Vessel Length in Woody Plants." *American Journal of Botany* 99: 1583–91.

Kannenberg, S. A., K. A. Novick, and R. P. Phillips. 2019. "Anisohydric Behavior Linked to Persistent Hydraulic Damage and Delayed Drought Recovery across Seven North American Tree Species." *New Phytologist* 222: 1862–72.

Klein, T., M. J. B. Zeppel, W. R. L. Anderegg, J. Bloemen, M. G. De Kauwe, P. Hudson, N. K. Ruehr, T. L. Powell, G. von Arx, and A. Nardini. 2018. "Xylem Embolism Refilling and Resilience against Drought-Induced Mortality in Woody Plants: Processes and Trade-Offs." *Ecological Research* 33: 839–55.

Konings, A. G., and P. Gentine. 2017. "Global Variations in Ecosystem-Scale Isohydricity." *Global Change Biology* 23: 891–905.

Kursar, T. A., B. M. Engelbrecht, A. Burke, M. T. Tyree, B. El Omari, and J. P. Giraldo. 2009. "Tolerance to Low Leaf Water Status of Tropical Tree Seedlings Is Related to Drought Performance and Distribution." *Functional Ecology* 23: 93–102.

Levionnois, S., S. Coste, E. Nicolini, C. Stahl, H. Morel, and P. Heuret. 2020. "Scaling of Petiole Anatomies, Mechanics and

Vasculatures with Leaf Size in the Widespread Neotropical Pioneer Tree Species *Cecropia obtusa* Trécul (Urticaceae)." *Tree Physiology* 40: 245–58.

Li, L., M. L. McCormack, C. Ma, D. Kong, Q. Zhang, X. Chen, Z. Hui, Ü. Niinemets, and D. Guo. 2015. "Leaf Economics and Hydraulic Traits Are Decoupled in Five Species-Rich Tropical-Subtropical Forests." *Ecology Letters* 18: 899–906.

Li, S., M. Feifel, Z. Karimi, B. Schuldt, B. Choat, and S. Jansen. 2015. "Leaf Gas Exchange Performance and the Lethal Water Potential of Five European Species during Drought." *Tree Physiology* 36: 179–92.

Li, W., X. Tian, H. Sheng, Y. Liu, and R. Zhang. 2019. "Effects of Drought Stress and re-Watering on Photosynthesis and Root Growth of *Phoebe chekiangensis*." *Ecological Science* 38: 182–8.

Li, X., J. Bao, J. Wang, C. Blackman, and D. Tissue. 2021. "Antecedent Drought Condition Affects Responses of Plant Physiology and Growth to Drought and Post-Drought Recovery." *Frontiers in Forests and Global Change* 4: 704470.

Lin, T.-C., S. P. Hamburg, K.-C. Lin, L.-J. Wang, C.-T. Chang, Y.-J. Hsia, M. A. Vadeboncoeur, G. M. M. McMullen, and C.-P. Liu. 2011. "Typhoon Disturbance and Forest Dynamics: Lessons from a Northwest Pacific Subtropical Forest." *Ecosystems* 14: 127–43.

Liu, B., Q. Liu, S. Daryanto, S. Guo, Z. Huang, Z. Wang, L. Wang, and X. Ma. 2018. "Responses of *Chinese Fir* and *Schima superba* Seedlings to Light Gradients: Implications for the Restoration of Mixed Broadleaf-Conifer Forests from Chinese Fir Monocultures." *Forest Ecology and Management* 419–420: 51–7.

Martínez-Vilalta, J., R. Poyatos, D. Aguadé, J. Retana, and M. Mencuccini. 2014. "A New Look at Water Transport Regulation in Plants." *New Phytologist* 204: 105–15.

Martin-StPaul, N., S. Delzon, and H. Cochard. 2017. "Plant Resistance to Drought Depends on Timely Stomatal Closure." *Ecology Letters* 20: 1437–47.

McAdam, S. A. M., and T. J. Brodribb. 2015. "The Evolution of Mechanisms Driving the Stomatal Response to Vapor Pressure Deficit." *Plant Physiology* 167: 833–43.

McDowell, N. G., R. A. Fisher, C. Xu, J. C. Domec, T. Hölttä, D. S. Mackay, J. S. Sperry, et al. 2013. "Evaluating Theories of Drought-Induced Vegetation Mortality Using a Multimodel–Experiment Framework." *New Phytologist* 200: 304–21.

McDowell, N. G., G. Sapes, A. Pivovaroff, H. D. Adams, C. D. Allen, W. R. L. Anderegg, M. Arend, et al. 2022. "Mechanisms of Woody-Plant Mortality under Rising Drought, CO_2 and Vapour Pressure Deficit." *Nature Reviews Earth & Environment* 3: 294–308.

Medlyn, B. E., M. G. De Kauwe, and R. A. Duursma. 2016. "New Developments in the Effort to Model Ecosystems under Water Stress." *New Phytologist* 212: 5–7.

Meinzer, F. C., and K. A. McCulloh. 2013. "Xylem Recovery from Drought-Induced Embolism: Where Is the Hydraulic Point of no Return?" *Tree Physiology* 33: 331–4.

Miyashita, K., S. Tanakamaru, T. Maitani, and K. Kimura. 2005. "Recovery Responses of Photosynthesis, Transpiration, and Stomatal Conductance in Kidney Bean Following Drought Stress." *Environmental and Experimental Botany* 53: 205–14.

Mursinna, A. R., E. McCormick, K. Van Horn, L. Sartin, and A. M. Matheny. 2018. "Plant Hydraulic Trait Covariation: A Global Meta-Analysis to Reduce Degrees of Freedom in Trait-Based Hydrologic Models." *Forests* 9: 446.

Ogle, K., J. J. Barber, C. Willson, and B. Thompson. 2009. "Hierarchical Statistical Modeling of Xylem Vulnerability to Cavitation." *New Phytologist* 182: 541–54.

Pan, Y., R. A. Birdsey, O. L. Phillips, and R. B. Jackson. 2013. "The Structure, Distribution, and Biomass of the world's Forests." *Annual Review of Ecology, Evolution, and Systematics* 44: 593–622.

Peguero-Pina, J., Ó. Mendoza-Herrer, E. Gil-Pelegrín, and D. Sancho-Knapik. 2018. "Cavitation Limits the Recovery of Gas Exchange after Severe Drought Stress in Holm Oak (*Quercus ilex* L.)." *Forests* 9: 443.

Pérez-Harguindeguy, N., S. Díaz, E. Garnier, S. Lavorel, H. Poorter, P. Jaureguiberry, M. S. Bret-Harte, et al. 2013. "New Handbook for Standardised Measurement of Plant Functional Traits Worldwide." *Australian Journal of Botany* 61: 167–234.

Pou, A., H. Medrano, M. Tomàs, S. Martorell, M. Ribas-Carbó, and J. Flexas. 2012. "Anisohydric Behaviour in Grapevines Results in Better Performance under Moderate Water Stress and Recovery than Isohydric Behaviour." *Plant and Soil* 359: 335–49.

R Core Team. 2018. *R: A Language and Environment for Statistical Computing*. Vienna: R Foundation for Statistical Computing. https://www.R-project.org/.

Roman, D. T., K. A. Novick, E. R. Brzostek, D. Dragoni, F. Rahman, and R. P. Phillips. 2015. "The Role of Isohydric and Anisohydric Species in Determining Ecosystem-Scale Response to Severe Drought." *Oecologia* 179: 641–54.

Schulte, P. J., and T. M. Hinckley. 1985. "A Comparison of Pressure-Volume Curve Data Analysis Techniques." *Journal of Experimental Botany* 36: 1590–602.

Shao, J. 2022. "Dataset of Drought-Rewatering Experiment on Five Subtropical Tree Species." Figshare, Data Set. https://doi.org/10.6084/m9.figshare.20326380.v1.

Sperry, J. S., J. R. Donnelly, and M. T. Tyree. 1988. "A Method for Measuring Hydraulic Conductivity and Embolism in Xylem." *Plant, Cell and Environment* 11: 35–40.

Trueba, S., R. Pan, C. Scoffoni, G. P. John, S. D. Davis, and L. Sack. 2019. "Thresholds for Leaf Damage Due to Dehydration: Declines of Hydraulic Function, Stomatal Conductance and Cellular Integrity Precede those for Photochemistry." *New Phytologist* 223: 134–49.

Urli, M., A. J. Porte, H. Cochard, Y. Guengant, R. Burlett, and S. Delzon. 2013. "Xylem Embolism Threshold for Catastrophic Hydraulic Failure in Angiosperm Trees." *Tree Physiology* 33: 672–83.

Vargas, R., O. Sonnentag, G. Abramowitz, A. Carrara, J. M. Chen, P. Ciais, A. Correia, et al. 2013. "Drought Influences the Accuracy of Simulated Ecosystem Fluxes: A Model-Data Meta-Analysis for Mediterranean Oak Woodlands." *Ecosystems* 16: 749–64.

Wang, S., R. M. Callaway, D.-W. Zhou, and J. Weiner. 2017. "Experience of Inundation or Drought Alters the Responses of Plants to Subsequent Water Conditions." *Journal of Ecology* 105: 176–87.

Xu, Z., G. Zhou, and H. Shimizu. 2010. "Plant Responses to Drought and Rewatering." *Plant Signaling and Behavior* 5: 649–54.

Yan, E.-R., X.-H. Wang, and J.-J. Huang. 2006. "Shifts in Plant Nutrient Use Strategies under Secondary Forest Succession." *Plant and Soil* 289: 187–97.

Yu, G., Z. Chen, S. Piao, C. Peng, P. Ciais, Q. Wang, X. Li, and X. Zhu. 2014. "High Carbon Dioxide Uptake by Subtropical Forest Ecosystems in the East Asian Monsoon Region." *Proceedings of the National Academy of Sciences* 111: 4910–5.

Yuan, W., W. Cai, Y. Chen, S. Liu, W. Dong, H. Zhang, G. Yu, et al. 2016. "Severe Summer Heatwave and Drought Strongly Reduced Carbon Uptake in Southern China." *Scientific Reports* 6: 18813.

Zhu, S.-D., Y.-J. Chen, Q. Ye, P.-C. He, H. Liu, R.-H. Li, P.-L. Fu, G.-F. Jiang, and K.-F. Cao. 2018. "Leaf Turgor Loss Point Is Correlated with Drought Tolerance and Leaf Carbon Economics Traits." *Tree Physiology* 38: 658–63.

Zhu, S.-D., R.-H. Li, P.-C. He, Z. Siddiq, K.-F. Cao, and Q. Ye. 2019. "Large Branch and Leaf Hydraulic Safety Margins in Subtropical Evergreen Broadleaved Forest." *Tree Physiology* 39: 1405–15.

SUPPORTING INFORMATION

Additional supporting information can be found online in the Supporting Information section at the end of this article.

How to cite this article: Shao, Junjiong, Xuhui Zhou, Peipei Zhang, Deping Zhai, Tengfei Yuan, Zhen Li, Yanghui He, and Nate G. McDowell. 2022. "Embolism Resistance Explains Mortality and Recovery of Five Subtropical Evergreen Broadleaf Trees to Persistent Drought." *Ecology* e3877. https://doi.org/10.1002/ecy.3877